Preparation of M−Al and M−Ca−Al (M: Sr, Cd, Ni, Ca, and Co) mixed oxides derived from LDH precursors as the high performance heterogeneous base catalysts for efficient synthesis of chalcones

Zahra Nazari[1] · Vahid Mahdavi[1,2] · Kaveh Khosravi[2,3]

Abstract

In this study, the catalytic activity of calcined M_3Al (M: Sr, Cd, Ni, Co, and Ca) and the effect of replacing divalent cations with Ca^{2+} in calcined $M_xCa_{3-x}Al$ hydrotalcite on the catalytic conversion of benzaldehyde and acetophenone to chalcone via Claisen–Schmidt condensation has been investigated. A series of M_3Al and $M_xCa_{3-x}Al$ were synthesized by the co-precipitation method and characterized by SEM, BET, FT-IR, EDS, XRD, CO_2-TPD techniques, and the Hammett indicator method. The results showed that the synthesized samples have normal surface area, high crystallinity, and three types of moderate, strong, and stronger basic sites. The catalytic activity is effectively dependent on the number of stronger alkaline sites. The effects of different parameters such as calcination temperature, solvents, catalyst amount, catalyst reusability, and the effects of electron-donating and electron-withdrawing groups were investigated. In optimum conditions over 0.04 wt% $Sr_{0.5}Ca_{2.5}Al$ catalyst, at atmospheric pressure, 60 °C, in ethanol, yield (%) of chalcone was achieved at 87%.

Graphical abstract
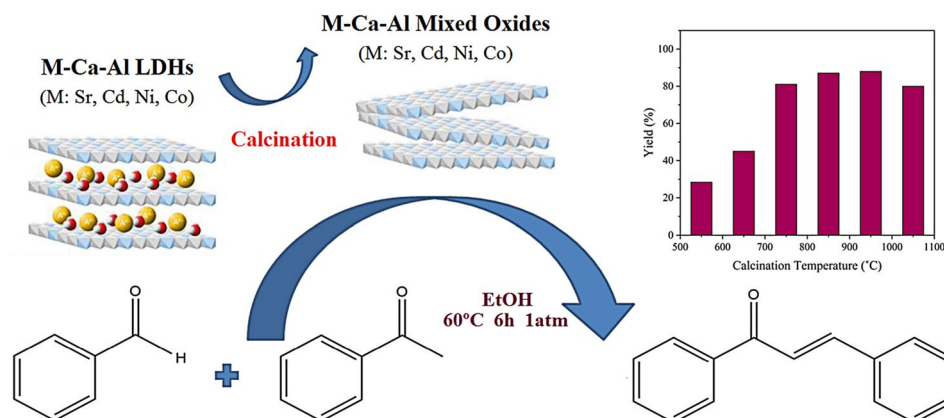
Keywords Solid base catalyst · Hydrotalcite · Mixed oxides · Chalcones synthesis · Claisen–Schmidt condensation

✉ Vahid Mahdavi
v-mahdavi@araku.ac.ir

1. Department of Chemistry, Surface Chemistry and Catalysis Division, Faculty of Science, Arak University, Arak 38156-8-8349, Iran

2. Institute of Nanoscience and Nanotechnology, Arak University, Arak 38156-8-8349, Iran

3. Department of Chemistry, Faculty of Science, Arak University, Arak 38156-8-8349, Iran

Introduction

Chalcone (1, 3-diaryl-2-propene-1-one) is an important group of organic compounds found in some plants or prepared synthetically [1–3]. Chalcones are aromatic ketones belonging to the flavonoid family [4, 5]. Chalcones are of great importance in biochemistry, and they are the starting material of many important biological compounds

[6–8]. They have important properties and wide biological activities [9] such as anti-fungal, antiviral, antioxidant, anti-inflammatory effects and anti-depressant activities, anti-cancer properties, anti-tubercular, anti-hyperglycemic agents [10–13], good antibacterial effects [14], and enzyme inhibitory properties [15, 16].

Commonly chalcone is obtained from the Claisen–Schmidt condensation between acetophenone and benzaldehyde [7, 17] in the presence of a base catalyst that is one of the important strategies for the development of carbon–carbon bonding [15]. Generally, alkaline hydroxides [18] are used as the homogeneous catalysts for this synthesis, which have many disadvantages [19]. Recently, due to the assumption of greener technologies for the synthesis of compounds, solid base catalysts are preferred over homogeneous ones. These catalysts have excellent activity and can be easily separated, revived, and reused [17, 20, 21].

Solid base catalysts have many different types, such as alkaline earth oxides and hydroxides, mixed oxides, clays, zeolites, hydrotalcites, etc. [22, 23]. Among the heterogeneous base catalysts, hydrotalcites are one of the most important ones due to their numerous applications. They are easily synthesized, have low cost, have a large surface area, and are widely used as base catalysts [24–26]. Hydrotalcites (HT), called layered double hydroxides (LDHs), have recently attracted much notice as new environmentally friendly catalysts [24, 27]. Reactions such as using LDH for biodiesel synthesis [22] and steam reforming of biomass [25], Claisen–Schmidt condensation [4, 28], Aldol condensation [29], Knoevenagel condensation [30], and Baeyer–Villiger oxidation of cyclohexanone to ε-caprolactone has been done [31].

LDHs can be depicted by the common formula: $[M^{2+}_{1-x}M^{3+}_x (OH)_2]^{x+}$. $A^{n-}_{x/n}$. zH_2O [32], where M^{2+} represents divalent metal cations, M^{3+} represents trivalent metal cations, and A^{n-} represents interspersed anions with charge n^- [32–34], so that water and anions are placed between the layers [28, 35]. $X = M^{3+}/(M^{2+} + M^{3+})$ the molar ratio for most hydrotalcites is about 0.2 until 0.33 [25, 36]. Various arrangements of divalent and trivalent cations have been used in the synthesis of LDHs that show many remarkable properties such as good basic character, vast surface area, thermally stable dispersion of metal ion components, high homogeneity, and contributory effects displayed between the elements [25, 37]. All divalent metals such as Co, Ca, Mg, Cd, Fe, Zn, and Ni form LDHs [38, 39]. LDHs prepared with Ca^{2+} cations have a low price, are non-toxic, have significant basic properties, and have very effective catalytic activity in many reactions. Mixed metal oxides derived from LDH precursors show good properties. During the calcination of LDH precursors hydroxyl groups are removed the interlayer structure of metal oxides and crystal shape are changed, causing an increase in specific surface area, expansion of mesoporosity, thermal stability, strong alkalinity, and enhanced adsorption capacity [28, 40–43].

In this work, we have prepared a new, recyclable, and deeply effective catalyst in the synthesis of chalcones under easy and green conditions using the Claisen–Schmidt condensation reaction. For this purpose, we synthesized and compared a series of M–Ca–Al (M = Sr, Ni, Cd, and Co) (with $(M^{2+} + Ca^{2+})/Al^{3+} = 3$) mixed metal oxides derived from LDH precursors as the heterogeneous solid base catalysts and they were used in chalcone synthesis via Claisen–Schmidt condensation between acetophenone and benzaldehyde as a model of C–C bond formation reaction. For the first time, we want to investigate how adding small amounts of other divalent cations (M^{2+}) to the usual hydrotalcite-like (Ca–Al) sample so that the ratio of divalent to trivalent cation remains constant affects the structure, basicity, and activity of the catalyst in the condensation reaction. All catalysts were characterized with FT-IR, FESEM, CO_2-TPD, BET, and XRD techniques, and the Hammett indicator method to investigate the relationship between catalytic performance, structure, and basicity of catalysts.

Experimental

Materials

Ethanol [C_2H_5OH (99%)], double deionized water (DDW), $Ni(NO_3)_2 \cdot 6H_2O$ (99%), $Sr(NO_3)_2 \cdot 4H_2O$ (99%), $Co(NO_3)_2 \cdot 6H_2O$ (97%), $Cd(NO_3)_2 \cdot 4H_2O$ (99%), Na_2CO_3 (> 99%), $Ca(NO_3)_2 \cdot 4H_2O$ (> 99%), $Al(NO_3)_3 \cdot 9H_2O$ (98.5%), benzaldehyde [C_6H_5CHO (98%)], and acetophenone [$C_6H_5C(O)CH3$ (99%)] were purchased from Merck Company. Ethanol [C_2H_5OH (96%)] was purchased from JATA Co.

Preparation of hydrotalcite-like catalysts

The hydrotalcite-like catalysts were synthesized by the co-precipitation method [22, 44]. In a typical method for the preparation of the Ca–Sr–Al hydrotalcite catalyst with (Ca + Sr)/Al molar ratio of (2.5 + 0.5)/1, at first, the solution of Na_2CO_3 (0.75 M) (solution A) and the common solution of $Ca(NO_3)_2 \cdot 4H_2O$, $Sr(NO_3)_2 \cdot 4H_2O$, and $Al (NO_3)_3 \cdot 9H_2O$ were prepared in deionized water (solution B). Then, both solutions were simultaneously poured into 50 mL of deionized water accompanied with vigorous mechanical stirring, maintaining the pH 10 at 65 °C. The blend was stirred vigorously for 20 h, then filtered and washed with deionized water several times to bring the pH to about 7–8. The precipitates were dried in an oven at 80 °C for 20 h and then calcined under airflow at 850 °C for 5 h. Also, calcined samples of hydrotalcite-like catalysts with the molar ratio of
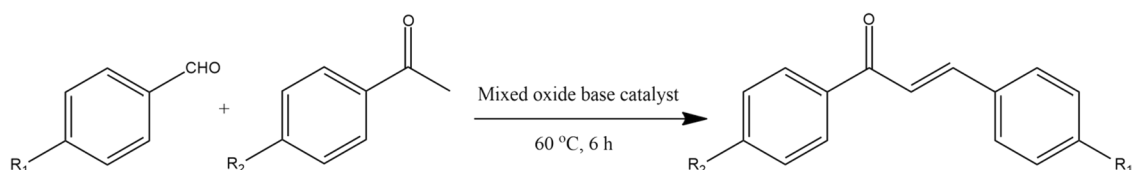
Scheme 1 Preparation of chalcone

$M^{2+}/M^{3+} = 3/1$ such as Ca_3Al, Ni_3Al, Cd_3Al, Sr_3Al, Co_3Al, $Sr_{0.125}Ca_{2.875}Al$, $Sr_{0.25}Ca_{2.75}Al$, $Sr_{0.75}Ca_{2.25}Al$, $Cd_{0.5}Ca_{2.5}Al$, $Co_{0.5}Ca_{2.5}Al$, and $Ni_{0.5}Ca_{2.5}Al$ were synthesized with this method.

Catalyst characterization

FESEM images were taken with a TESCAN instrument model MIRA III. The energy-dispersive spectroscopy (EDS) of samples was also recorded with this device. BET surface area of the catalytic samples from the nitrogen adsorption–desorption isotherms was recorded in the BELSORP MINI II device. The samples were degassed for 2 h at 300 °C before measurement. The alkalinity of the catalysts was evaluated by CO_2-TPD (Carbon dioxide temperature programmed desorption). A Micromeritics instrument (model Chemisorb 2750) was used for CO_2-TPD within a temperature range of 100–1000 °C under helium flow (20 mL min^{-1}) and released CO_2 was detected by a TCD detector. X-ray diffraction (XRD) was utilized to investigate the structure of the catalysts. A Philips diffractometer was used to generate the diffraction patterns with Cu Kα radiation (Model PW 1800). The basicity of the catalysts was evaluated by CO_2-TPD (carbon dioxide temperature programmed desorption). A Micromeritics instrument (model Chemisorb 2750) was used for CO_2-TPD under helium flow (20 mL min^{-1}) in the temperature range of 100–1000 °C, and released CO_2 was detected by a TCD detector. FT-IR spectra of catalysts were obtained using KBr pellets on a BRUKERALPHA FT-IR spectrometer.

The Hammett indicator method was utilized to determine the alkaline strength of the synthesized catalysts. According to the procedure of our previous articles [45] para nitroaniline (H_ = 18.4), alizarin yellow R (H_ = 11.0), 4-chloro-2-nitroaniline (H_ = 17.7), 2, 4-dinitroaniline (H_ = 15.0), and phenolphthalein (H_ = 9.8) Hammett indicators are used in our tests.

Catalytic tests and activity evaluation

The reaction was done in the liquid phase in a batch reactor consisting of a round bottom flask with two necks, a sampling apparatus, and a condenser. According to Scheme 1, a typical reaction mixture containing acetophenone (10 mmol), benzaldehyde (12 mmol), and ethanol as a solvent was heated in an oil bath to 60 °C. Then, 0.04 wt% (0.09 g) of the catalyst was added to the flask after reaching the desired temperature. The reaction mixture was stirred at a rate of 1200 cycles/min with a magnetic stirrer for 6 h. The reaction process was checked with TLC.

After the completion of the reaction, the catalyst was separated from the hot reaction mixture by filtration. Then, the reaction mixture was cooled to 20 °C and the solid product (chalcone) was separated from the blend by filtration. The remaining solution was injected into a GC (Perkin Elmer 8500) with an FID detector and 3% DEXIL 300 column to determine the amount of residual benzaldehyde. The conversion percentage was calculated based on benzaldehyde in the final reaction mixture according to the following equation:

$$\text{Conversion (\%)} = \frac{\text{moles of benzaldehyde reacted}}{\text{Initial moles of benzaldehyde}} \times 100 \tag{1}$$

The chalcone product was separated from the reaction mixture (at 20 °C), recrystallized by the two-solvent (hot ethanol and cold H_2O) method, and weighed [13, 46].

Melting point technique, FT-IR(BRUKERALPHA), ^{13}C-NMR, and ^1H-NMR (BRUKER-AVANCe 300 NMR-300 MHz Spectrometry) spectra were used to identify chalcone compounds. The yield % of the product was calculated as follows:

$$\text{Yield (\%)} = \frac{\text{Amount of produced chalcone}}{\text{Theoritical value}} \times 100 \tag{2}$$

Results and discussion

Catalysts characterization

XRD

The X-ray diffraction patterns of the two-component M/Al (M: Ca, Ni, Cd, Co, and Sr) with $M^{2+}/Al^{3+} = 3/1$ and three-component M/Ca/Al (M: Ni, Cd, Co, and Sr) HT-like catalyst samples with $(M^{2+} + Ca^{2+})/Al^{3+} = 3/1$ molar ratio after calcination are shown in Fig. 1. Also, the XRD pattern of Ca_3Al sample before calcination is reported in Fig. 1a.
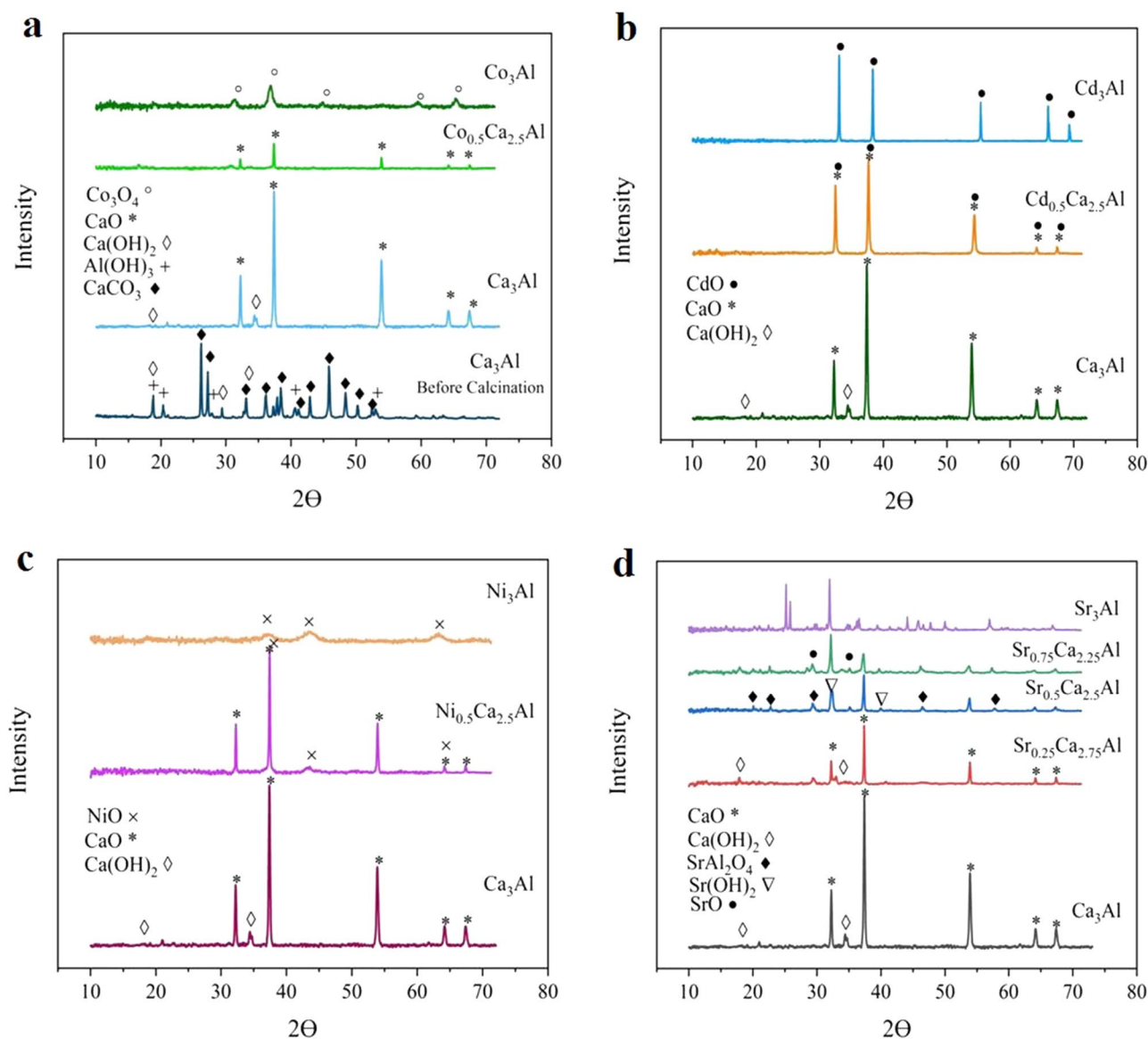
Fig. 1 XRD patterns of the catalyst samples: **a** Ca_3Al before calcination and Ca_3Al, $Co_{0.5}Ca_{2.5}Al$, Co_3Al after calcination **b** Ca_3Al, $Cd_{0.5}Ca_{2.5}Al$, Cd_3Al, **c** Ca_3Al, $Ni_{0.5}Ca_{2.5}Al$, Ni_3Al, **d** Ca_3Al, $Sr_{0.25}Ca_{2.75}Al$, $Sr_{0.5}Ca_{2.5}Al$, $Sr_{0.75}Ca_{2.25}Al$, Sr_3Al after calcinations

This pattern is related to peaks of $CaCO_3$, $Al(OH)_3$, and $Ca(OH)_2$ phases according to standard cards (00-041-1475, 01-074-1119, 00-044-1481) which confirm the hydrotalcite-like structure of Ca_3Al before calcination [24, 47]. According to Fig. 1, results showed that the calcined hydrotalcites are of relatively high crystallinity which agrees with the previous studies [40–42]. In all the calcined samples, the XRD pattern of calcium oxide was clearly observed, and the diffraction peaks at 2θ: 32.33, 37.38, 53.78, 64.1, and 67.29° were related to the presence of CaO phase according to the standard card (01-077-2376) [47, 48]. Also, the peaks were attributed to the $Ca(OH)_2$ phase in 2θ: 17.96, and 34 were identified in the Sr/Ca/Al and $Co_{0.5}Ca_{2.5}Al$ samples

according to the standard card (00-044-1481) [47, 48]. There is no diffraction line for the alumina phases. Al^{3+} cations can be completely incorporated into the CaO framework or may form an amorphous AlO_x phase. The presence of aluminum in the structure of HT-like catalytic samples causes a change in the reflection to a higher 2θ [47]. Also, in the two-component M/Al samples, the NiO, CdO, and Co_3O_4 phases were observed according to standard cards (01-1239), (01-075-0596), and (74-1656), respectively [49].

But in the containing strontium samples, peaks related to SrO, $SrAl_2O_4$, and $Sr(OH)_2$ phases are observed according to standard cards (00-006-0520) and (00-027-0847), respectively. As the amount of strontium in the samples

Table 1 Textural properties of catalyst samples

| Catalysts	Total pore volume[a] (cm^3 g^{-1})	SBET[b] (m^2 g^{-1})	Average pore size[c] (nm)	Particle size[d] (nm)
Ca3Al	0.06	39	5.94	35.72
Co0.5Ca2.5Al	0.04	6	26.63	61.65
Ni0.5Ca2.5Al	0.17	33	20.54	57.16
Cd0.5Ca2.5Al	0.10	18	22.99	35.85
Sr0.5Ca2.5Al	0.05	14	16.08	42.36

[a], [b]Calculated from BET method. [c]Calculated from BJH plot. [d]Calculated from Scherer's equation

increases, these peaks become sharper, and the peaks related to calcium oxide decrease. The peaks related to the $SrAl_2O_4$ phase at 2θ: 20.1, 22.8, 29.4, 35.2, 46.45, and 57.68 degrees were determined according to the standard card (00-034-0379). The average crystal size of these catalyst samples was calculated from X-ray diffraction using Scherer's equation, which is reported in Table 1. Also, the XRD pattern of the $Sr_{0.5}Ca_{2.5}Al$ sample before calcination (Fig. was not reported) confirms the hydrotalcite-like structure and shows the peaks related to calcium carbonate, strontium carbonate, $(Sr, Ca)CO_3$, $Sr(OH)_2$ and $Al(OH)_3$ phases according to standard cards (01-086-2341, 01-071-2393, 00-044-1421, 01-074-1119). In the $Sr_{0.5}Ca_{2.5}Al$ sample after calcination, the peaks related to carbonate phases are completely lost and only some peaks related to $Sr(OH)_2$ are observed.

FT-IR

The FT-IR spectra of the Ca_3Al catalyst before and after calcination at 750 °C are shown in Fig. 2a. The FT-IR spectra of the sample before calcination confirm the hydrotalcite-like structure and show water molecules in the structure of the catalyst with peaks in the range of 3630–3430 cm^{-1}, which belongs to O–H stretching vibrations. Also, the presence of a peak in the region of 3700 cm^{-1} indicates the OH group and the presence of metal hydroxide. A wide and strong peak is also observed in the area of 1887–1384 cm^{-1}, which belongs to the carbonate group. In the FT-IR spectra of the Ca_3Al sample after calcination (Fig. 2a and b), the intensity of this peak is reduced and the peak related to H_2O stretching vibrations disappeared. The FT-IR spectra of all catalysts show that peaks are observed in the 3643 cm^{-1} region related to the OH group which remains inter layers of HT samples after calcination [50]. Also, in the range of 500–1000 cm^{-1} peaks related to metal oxides are observed (Fig. 2b) [51, 52].

BET and BJH analysis To determine the porosity and the structural properties of catalysts, the BET technique was used for all samples, and the results are presented in Fig. 3. According to Fig. 3a, the adsorption–desorption isotherm of
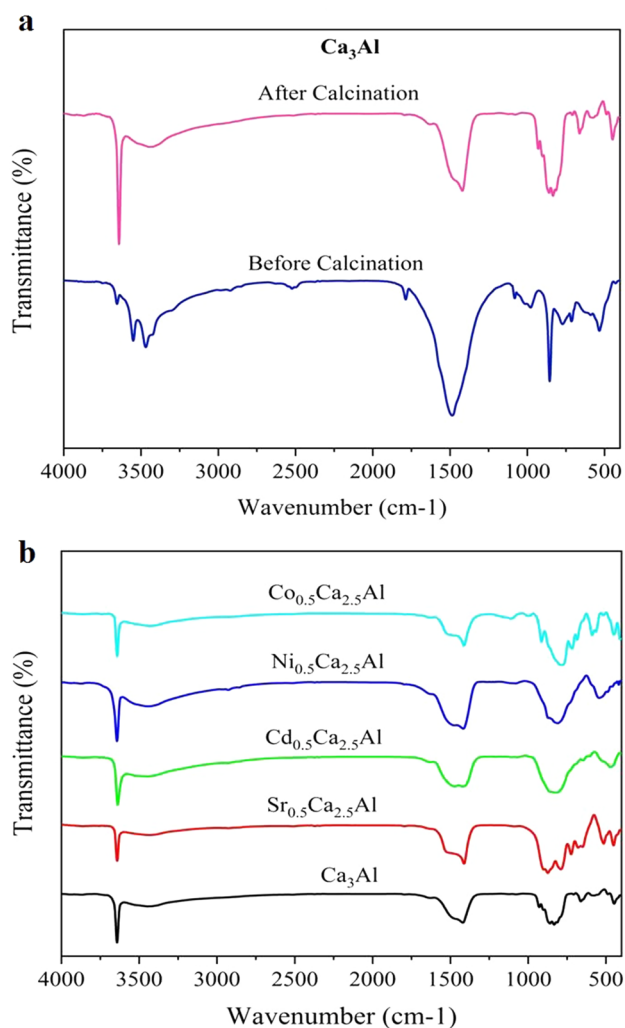
Fig. 2 a FT-IR of Ca_3Al catalyst before and after calcination at 750 °C **b** FT-IR of Ca_3Al and $M_{0.5}Ca_{2.5}Al$ catalysts (M: Ni, Cd, Co, and Sr) after calcination

the $Co_{0.5}Ca_{2.5}Al$ sample corresponds to type II and H2 hysteresis loop which is related to micropores materials with poorly adsorbed-adsorbent interaction. The $Ni_{0.5}Ca_{2.5}Al$ sample isotherm is approximately type V or (IV) with an H3 hysteresis loop in the range of 0.4–1 P/P°, indicating mesoporous structures and strip pores. Other catalysts show a mixture of type V and type II isotherms with an H2 and H3 hysteresis loop in the range of 0.75–1 P/P°, which confirms the presence of microporous-mesoporous structures. Also, Fig. 3b determines the pore size distribution profiles of the catalytic samples using the BJH method. As it is clear from Fig. 3b, the pore size distribution profiles of Ca_3Al and $Co_{0.5}Ca_{2.5}Al$ samples are different compared to other samples the pore size (r_p) corresponding to the maximum of curves is about 1.2 nm. Also, the average pore size of Ca_3Al is about 5.9414 nm and it has increased with the introduction of the third metal.
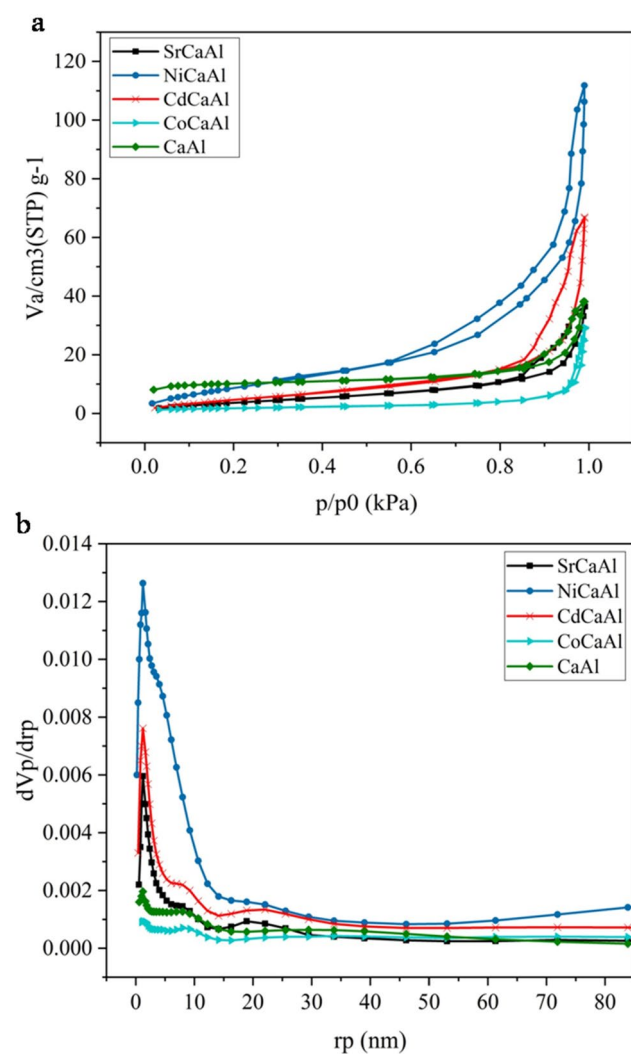
Fig. 3 a The absorption and desorption diagram, obtained from the BET analysis of Ca$_3$Al and M$_{0.5}$Ca$_{2.5}$Al catalysts (M: Ni, Cd, Co, and Sr) after calcination, **b** BJH plot of synthesized catalysts

The values of BET surface areas, pore volumes, and pore diameters of Ca$_3$Al, Sr$_{0.5}$Ca$_{2.5}$Al, Cd$_{0.5}$Ca$_{2.5}$Al, Co$_{0.5}$Ca$_{2.5}$Al, and Ni$_{0.5}$Ca$_{2.5}$Al calcined HT-like catalysts are reported in Table 1. According to Table 1, the surface area of the Ca$_3$Al sample is 39 m^2/g, which is in good agreement with the surface values for calcined HT samples reported in the literature [53]. Table 1 funds that replacing a small amount of calcium with another divalent metal has caused a decrease in the BET surface area so that the Co$_{0.5}$Ca$_{2.5}$Al sample has the lowest surface area (6 m^2/g). Also, the total pore volumes of catalyst samples are about 0.04–0.17 cm^3 g^{-1} and the nickel-containing catalyst has the largest pore volume.

FESEM and EDS The FESEM images of all catalytic samples are given in Fig. 4, in order to compare the morphology of the prepared catalysts. According to Fig. 4, the morphol-

ogy of the catalyst samples has changed significantly with the replacement of the divalent cations. FESEM results also show the agglomerated nanoparticles with a size of 30–52 nm which is consistent with the data from the XRD pattern.

Also, the XDS analysis was utilized to determine the chemical composition of the surface of catalyst samples (Fig. 5, Table 2). The results show that the percentage composition of the elements on the surface of the catalyst is almost the same as the bulk and confirms the homogeneity of the percentage composition in the whole sample.

Mapping analysis was used to determine the abundance of Sr, Ca, and Al elements on the surface of the Sr$_{0.5}$Ca$_{2.5}$Al catalyst and the scatter map of element distribution, the results of which are shown in Fig. 6. Based on that, the distribution of elements on the surface is uniform and homogeneous, and accumulation is not seen.
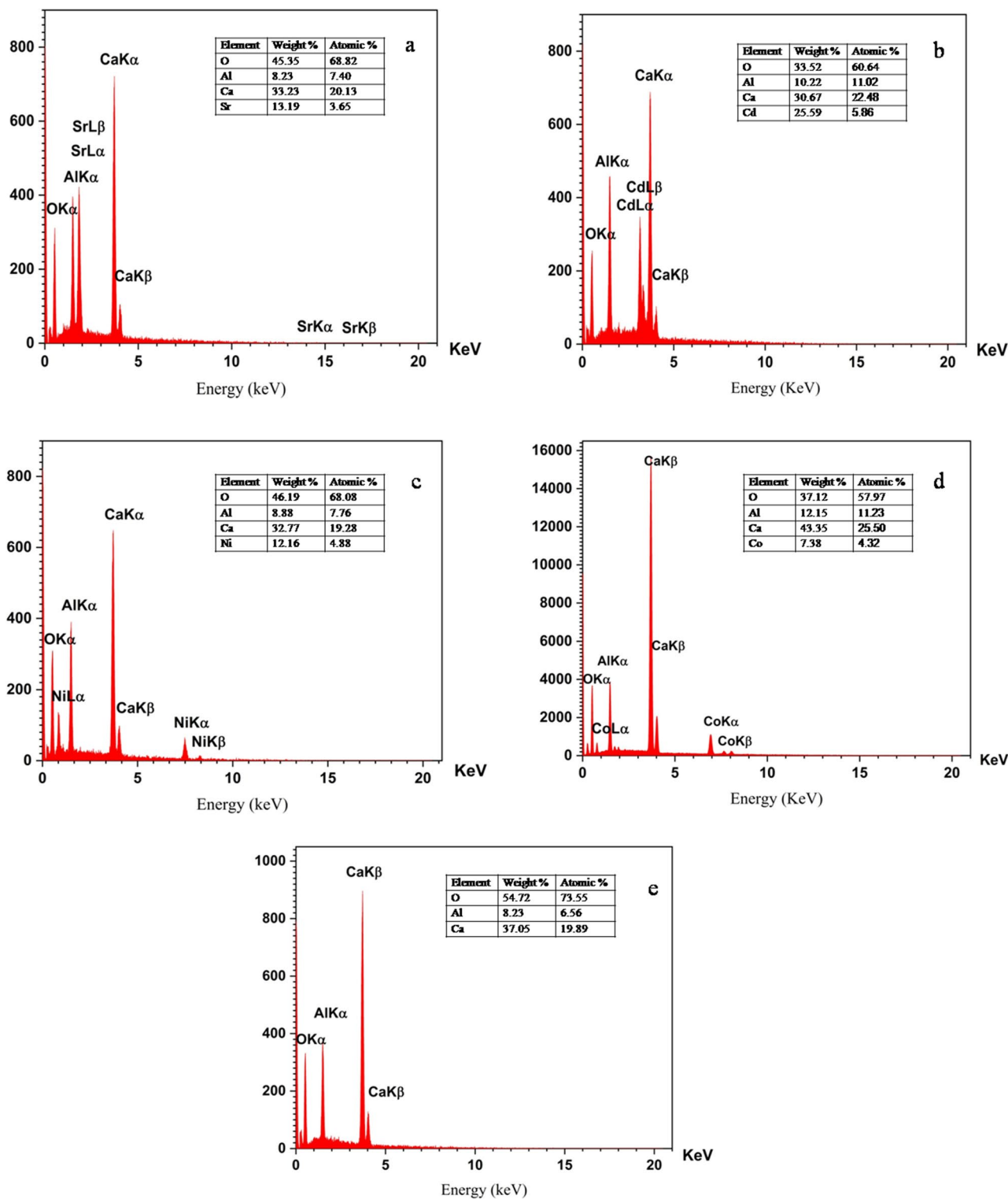
CO$_2$-TPD

In order to evaluate the surface basic strength and determine the number of alkaline sites on the surface of the prepared catalysts, the CO$_2$-TPD technique was used for all samples after calcination, the results of which are shown in Fig. 7 and Table 3. In general, in the CO$_2$-TPD profiles, the number of peaks, the areas of peaks, and the position of peaks indicate the number of alkaline sites, the types of alkaline sites, and the strength of basic sites, respectively. Therefore, we can classify basic sites as medium, strong, and stronger sites according to the maximum desorption temperature of the desorption peaks. According to Fig. 7, the calcined Ca$_3$Al HT-like sample shows two CO$_2$ desorption peaks at around 426 and 720 °C, which indicates strong basic sites corresponding to Ca^{2+}–O^{2-} pairs. Also, calcined Ni$_{0.5}$Ca$_{2.5}$Al and Cd$_{0.5}$Ca$_{2.5}$Al samples, like sample Ca$_3$Al, show peaks with maximum temperatures of 563 °C, 727 °C, and 497 °C, 736 °C, respectively, which are related to strong alkaline sites. According to Fig. 7, the calcined Co$_{0.5}$Ca$_{2.5}$Al HT-like sample has two peaks at maximum temperatures of 246 and 716 °C, which correspond to medium and strong basic sites, respectively.

For the calcined Sr$_{0.5}$Ca$_{2.5}$Al HT-like sample, three desorption peaks have appeared at 497, 687, and 882 °C which peaks are related to strong and stronger base sites, respectively. According to XRD results (Fig. 1), the calcined sample content CaO, Sr(OH)$_2$, SrO, and SrAl$_2$O$_4$ phases. In this sample, the peaks corresponding to the temperatures of 497 and 687 °C match to basic sites of Sr(OH)$_2$ and CaO components, which have shifted from 426 to 497 °C and 720 to 678 °C due to the interaction with the other components. It seems that the desorption peaks at higher temperatures in the range of 700–850 °C are related to SrO and SrAl$_2$O$_4$ phases.
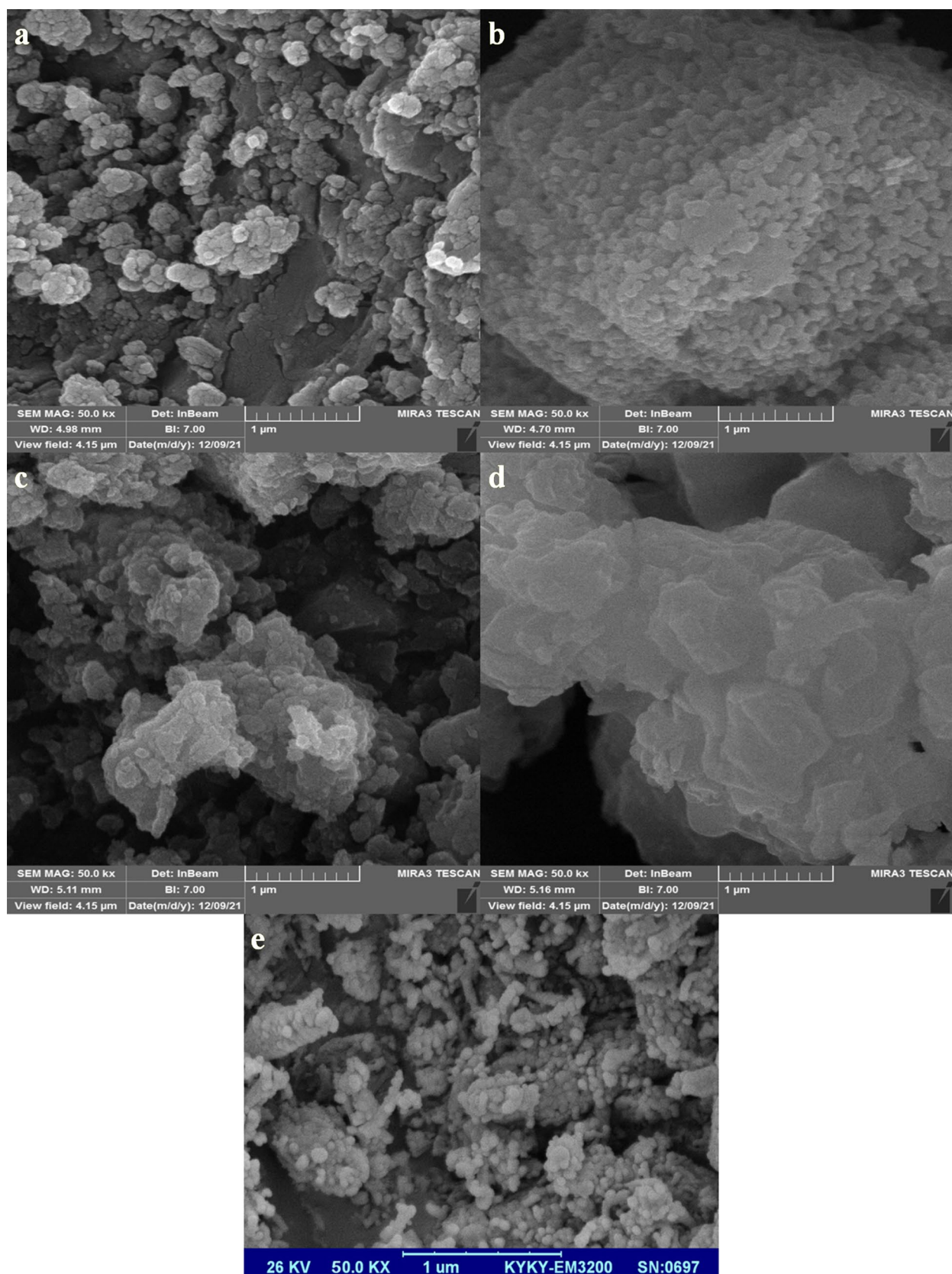
Fig. 4 FESEM images of the catalysts: **a** $Sr_{0.5}Ca_{2.5}Al$, **b** $Cd_{0.5}Ca_{2.5}Al$, **c** $Ni_{0.5}Ca_{2.5}Al$, **d** $Co_{0.5}Ca_{2.5}Al$, **e** Ca_3Al after calcination

Figure a table:

Element	Weight %	Atomic %
O	45.35	68.82
Al	8.23	7.40
Ca	33.23	20.13
Sr	13.19	3.65

Figure b table:

Element	Weight %	Atomic %
O	33.52	60.64
Al	10.22	11.02
Ca	30.67	22.48
Cd	25.59	5.86

Figure c table:

Element	Weight %	Atomic %
O	46.19	68.08
Al	8.88	7.76
Ca	32.77	19.28
Ni	12.16	4.88

Figure d table:

Element	Weight %	Atomic %
O	37.12	57.97
Al	12.15	11.23
Ca	43.35	25.50
Co	7.38	4.32

Figure e table:

Element	Weight %	Atomic %
O	54.72	73.55
Al	8.23	6.56
Ca	37.05	19.89

Fig. 5 EDS spectroscopy of the catalyst samples: **a** $Sr_{0.5}Ca_{2.5}Al$, **b** $Cd_{0.5}Ca_{2.5}Al$, **c** $Ni_{0.5}Ca_{2.5}Al$, **d** $Co_{0.5}Ca_{2.5}Al$, **e** Ca_3Al after calcination

The peak with a maximum temperature of 800 is related to the isolated oxygen species [54].

Hammett indicator method In order to evaluate the basic strengths (H_) of, Ca_3Al, $Ni_{0.5}Ca_{2.5}Al$, $Cd_{0.5}Ca_{2.5}Al$, $Co_{0.5}Ca_{2.5}Al$, $Sr_{0.125}Ca_{2.875}Al$, $Sr_{0.25}Ca_{2.75}Al$, $Sr_{0.5}Ca_{2.5}Al$, and $Sr_{0.75}Ca_{2.25}Al$ HT-like catalysts, the Hammett indicator

Table 2 Comparison of the M^{2+}/Al^{3+} molar ratio theoretical and experimental

Catalysts	Molar ratio of M^{2+}/Al^{3+}	
	Theoretical	Calculated from EDS
Ca_3Al	3: 1	3.03: 1
$Co_{0.5}Ca_{2.5}Al$	(0.5 + 2.5): 1	(0.28 + 2.40): 1
$Ni_{0.5}Ca_{2.5}Al$	(0.5 + 2.5): 1	(0.63 + 2.48): 1
$Cd_{0.5}Ca_{2.5}Al$	(0.5 + 2.5): 1	(0.61 + 2.01): 1
$Sr_{0.5}Ca_{2.5}Al$	(0.5 + 2.5): 1	(0.49 + 2.72): 1

procedure was also used, the results of which are shown in Table 3. In this experiment, the mixture of solid base sample and methanol was titrated by benzoic acid in the presence of indicators. In the Hammett method, catalysts with weaker alkaline strength than the strongest indicators do not change color, but catalysts with stronger alkaline strength than the weakest indicators change color [24]. From Table 3, it was found that Ca_3Al, $Ni_{0.5}Ca_{2.5}Al$, and $Cd_{0.5}Ca_{2.5}Al$ catalysts changed color in the presence of all indicators except for para nitroaniline and 4-chloro-2-nitroaniline. The $Co_{0.5}Ca_{2.5}Al$ catalyst changed color with phenolphthalein and alizarin yellow R, but did not change color with 2,4-dinitroaniline, 4- chloro-2-nitroaniline, and para nitroaniline. Catalysts containing strontium did not change color with phenolphthalein, and para nitroaniline. Also, the bimetallic catalysts of Ni_3Al, Cd_3Al, and Co_3Al did not change color with these alkaline reagents and could not be investigated by this method. Therefore, the alkaline strength (H_) of the Ca_3Al, $Ni_{0.5}Ca_{2.5}Al$, and $Cd_{0.5}Ca_{2.5}Al$, catalyst samples could be empirically denoted as $9.8 < H\_ < 17.7$. The basic strength of Sr_3Al, $Sr_{0.125}Ca_{2.875}Al$, $Sr_{0.25}Ca_{2.75}Al$, $Sr_{0.5}Ca_{2.5}Al$, $Sr_{0.75}Ca_{2.25}Al$, and $Co_{0.5}Ca_{2.5}Al$ could be empirically denoted as $11 < H\_ < 18.4$ and $9.8 < H\_ < 15$, respectively.

Catalytic performance

To evaluate the catalytic performance of calcined HT-like samples, the Claisen–Schmidt condensation reaction between acetophenone and benzaldehyde for the chalcone synthesis was studied as a model of the C–C bond formation reaction. The results are given in Table 3. According to the analysis of the ^1H-NMR spectra of the reaction product (spectra not shown), only the trans-chalcone configuration (E isomer) was obtained. Therefore, the percentage of selectivity in all runs was 100%. According to Table 3, the chalcone synthesis reaction was carried out in the presence of bimetallic calcined HT compounds such as Ca_3Al, Sr_3Al, Cd_3Al, Ni_3Al, and Co_3Al and trimetallic calcined hydrotalcite catalysts after calcination, and in the absence of a catalyst. According to Table 3, in the absence of a catalyst, benzaldehyde conversion (%) was

very little. Also, the Ca_3Al was the most efficient among the binary catalysts and the lowest product was obtained in the presence of the Co_3Al sample. In the presence of a calcined binary Ca_3Al HT-like sample, the yield (%) of chalcone was 61% (conversion 65.1(%)) and the yield (%) of chalcone in the presence of the $Co_{0.5}Ca_{2.5}Al$ catalyst decreased to 38% (conversion 38.2(%)). In the presence of $Ni_{0.5}Ca_{2.5}Al$ and $Cd_{0.5}Ca_{2.5}Al$ catalysts, the yield (%)/ conversion (%) have changed to 70.1/72, and 79.8/80.2%, respectively. Also, in the presence of the $Sr_{0.5}Ca_{2.5}Al$ catalyst yield (%) and conversion (%) have changed to 87.1% and 89.1, respectively. It seems that the replacement of calcium by cobalt has caused a decrease in the yield (%), and the replacement of calcium by Ni, Cd, and Sr, has caused an increase in the yield (%) of chalcone. To justify the difference in the performance of the synthesized catalysts, the results of CO_2-TPD analysis obtained from the area of the corresponding peaks (calculated using Origin Pro software) are shown in Table 3. According to Table 3, the synthesized catalysts in three temperature ranges: $T_{max} < 550$ °C, 550 °C $< T_{max} < 750$ °C, and 750 °C $< T_{max} < 950$ °C show the CO_2 desorption peaks (mmol $CO_2 \cdot g^{-1}$) which are related to medium, strong, and stronger basic sites. The Ca_3Al and $Co_{0.5}Ca_{2.5}Al$ catalysts do have not any stronger basic sites and for this reason, in their presence, the yield (%) of the chalcone is lower than other samples. Also, according to the results in Table 1, the BET surface area of the $Co_{0.5}Ca_{2.5}Al$ sample (6.2 $m^2 \cdot g^{-1}$) is much lower than the Ca_3Al surface area (39.4 $m^2 \cdot g^{-1}$) and has caused to decrease in the yield (%) of chalcone. According to Table 3, activity, yield (%) of chalcone, and conversion % of benzaldehyde in the presence of $Ni_{0.5}Ca_{2.5}Al$, $Cd_{0.5}Ca_{2.5}Al$, and $Sr_{0.5}Ca_{2.5}Al$ catalyst samples have increased with the increase in the stronger basic site. These results indicate that the catalytic activity is strongly related to the number of stronger basic sites and the activity value of more alkaline catalysts is higher than others. Therefore, the $Sr_{0.5}Ca_{2.5}Al$ catalyst has more millimoles of stronger basic sites (1.27 mmol $CO_2 \cdot g^{-1}$) than the other samples and therefore has more activity in this reaction. Also, in Table 3, the effect of the Sr/Ca molar ratio on the activity of Sr-containing catalyst samples was investigated. The samples of $Sr_{0.125}Ca_{2.875}Al$, $Sr_{0.25}Ca_{2.75}Al$, and $Sr_{0.75}Ca_{2.25}Al$ have shown almost the same catalytic activity compared to the $Sr_{0.5}Ca_{2.5}Al$ sample. Therefore, the $Sr_{0.5}Ca_{2.5}Al$ sample was chosen as a suitable solid base catalyst and used in further investigations. The performance of $Sr_{0.5}Ca_{2.5}Al$ HT-like before calcination also is given in Table 3. The results showed that this catalyst had a lower catalytic performance in this reaction compared to the mixed oxide sample obtained from it (after calcination). It was not completely stable and slightly dissolved in the reaction mixture causing leaching. In fact, based on the
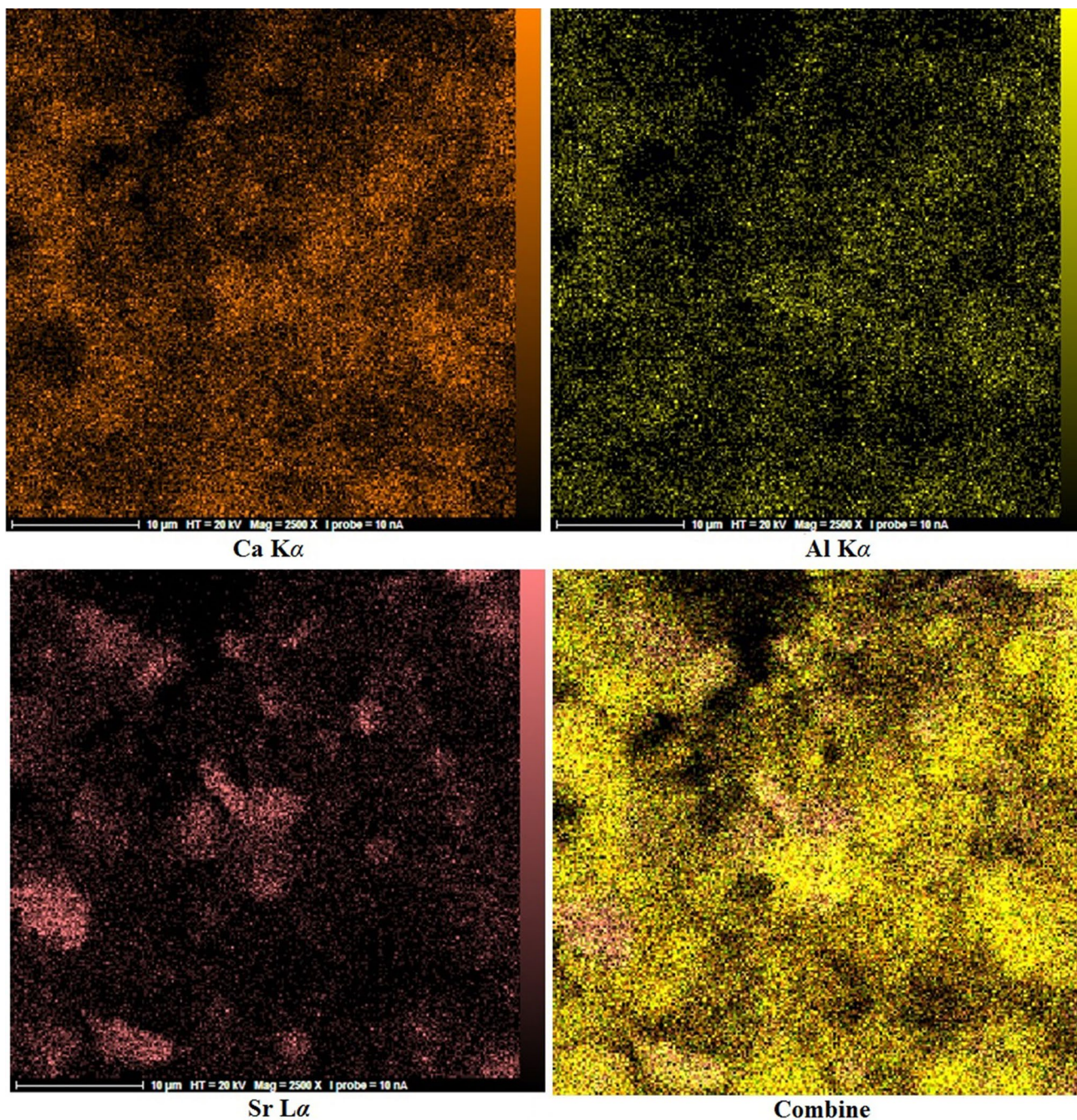
Fig. 6 Mapping of $Sr_{0.5}Ca_{2.5}Al$ catalyst after calcination

characterization results, the replacement of calcium by Ni, Cd, or Sr in the structure of calcined binary Ca_3Al HT-like catalyst, produces significant changes in basic strength, phase composition, morphology, and textural properties. So that $Sr_{0.5}Ca_{2.5}Al$ sample with CO_2 desorption peak in the temperature range of $750\ °C < T_{max} < 950\ °C$, contains very strong alkaline sites and phase composition of SrO, $SrAl_2O_4$, and $Sr(OH)_2$. The collection of these alterations should be caused by the observed difference in activity.

Therefore, the $Sr_{0.5}Ca_{2.5}Al$ sample has an acceptable performance in this reaction and was used as a suitable base catalyst in further detailed studies.

Effect of calcination temperature on the activity of the catalyst

Since suitable active sites are created in the catalyst during the calcination, this process is of special importance and
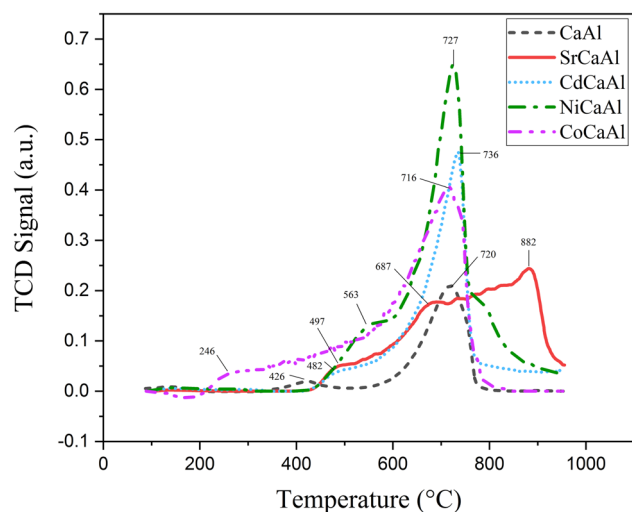
Fig. 7 CO_2-TPD of Ca_3Al and $M_{0.5}Ca_{2.5}Al$ catalysts (M: Ni, Cd, Co, and Sr) after calcination

the calcination conditions should be investigated experimentally. Figure 8 shows the yield (%) of chalcone produced in the presence of the $Sr_{0.5}Ca_{2.5}Al$ catalyst with different calcination temperatures (550–1050 °C) within 5 h. According to Fig. 8, the chalcone yield (%) is low in the presence of calcined $Sr_{0.5}Ca_{2.5}Al$ at 550 °C, and enhancement of the calcination temperature)550–850 °C(has increased the

chalcone yield (%) to 90%. But by raising the temperature to 1050 °C, the yield (%) of chalcone has decreased. Therefore, the calcination conditions (850 °C, 5 h) are appropriate for $Sr_{0.5}Ca_{2.5}Al$ HT-like catalyst due to the complete decomposition of precursor and the production of crystalline phases of SrO, CaO, and $SrAl_2O_4$ and the yield (%) of chalcone is maximum. In the 850–1050 °C temperature range, the crystalline phases of the catalyst sample may have been agglomerated due to the sintering effect.

Effect of the amount of catalyst

To investigate the effect of the amount of catalyst on the yield (%) of chalcone, the reactions were carried out in the presence of calcined $Sr_{0.5}Ca_{2.5}Al$ in the range of 0.009–0.05% (based on the mass of total raw material) at 60 °C for 6 h, benzaldehyde/acetophenone: 1.2, and 5 mL solvent (ethanol 96%). Also, the reaction was carried out without a catalyst which did not have significant efficiency. The results in Fig. 9a show that by increasing the amount of catalyst up to 0.04%, the yield (%) of the product increases to 87% and after that, the yield (%) decreases with a further increase in the catalyst amount. At first, by increasing the catalyst amount, the number of accessible active sites has increased therefore, the yield (%) of chalcone has increased. The reaction rate depends on the external surface. However, above 0.04 wt% (0.09 g), the diffusion rate of the raw

Table 3 Claisen–Schmidt condensation reaction and basic properties of the synthesized catalysts

Catalyst	Base strength[a] (H_)	Basic site[b] (mmol CO_2 g^{-1})				Conversion[c] (%)	Yield[d] (%) Of Chalcone	Activity[f] (h^{-1})
		$T_{max} < 550$ °C	$550 < T$°C$ < 750$	$750 < T$ °C$ < 950$	Total			
Ca_3Al	$9.8 < H\_ < 17.7$	0.19	2.08	–	2.27	65.1	61.2	3.50
$Co_{0.5}Ca_{2.5}Al$	$9.8 < H\_ < 15$	3.33	2.18	–	5.51	38.2	37.9	2.17
$Ni_{0.5}Ca_{2.5}Al$	$9.8 < H\_ < 17.7$	2.08	2.63	0.63	5.34	72	70.1	4
$Cd_{0.5}Ca_{2.5}Al$	$9.8 < H\_ < 17.7$	0.74	2.51	0.71	3.96	80.2	79.8	4.56
$Sr_{0.5}Ca_{2.5}Al$	$11 < H\_ < 18.4$	0.88	2.83	1.27	4.98	89.1	87.1	4.98
$Sr_{0.125}Ca_{2.875}Al$	$11 < H\_ < 18.4$	–	–	–	–	82.9	83.7	4.78
$Sr_{0.25}Ca_{2.75}Al$	$11 < H\_ < 18.4$	–	–	–	–	86.2	84.7	4.84
$Sr_{0.75}Ca_{2.25}Al$	$11 < H\_ < 18.4$	–	–	–	–	93	90	5.14
$Sr_{0.5}Ca_{2.5}Al$ (before calcination)	$9.8 < H\_ < 18.4$					67.2	66.1	3.77
Sr_3Al	$11 < H\_ < 18.4$	–	–	–	–	52.5	49.7	2.84
Cd_3Al	–	–	–	–	–	30.2	28.1	1.60
Ni_3Al	–	–	–	–	–	29.7	27.5	1.57
Co_3Al	–	–	–	–	–	7	–	–
Without Catalyst	–	–	–	–	–	4	–	–

[a]Has been achieved from the Hammett method. [b]Has been achieved from CO2-TPD. [c]Conversion percentage was calculated based on the decrease of the initial benzaldehyde in the reaction. [d]Yield of pure isolated product, [e]Gram of product per gram of catalyst in 1 h. Reaction conditions: 0.04 wt% of calcined catalyst at 850 °C, 5 mL solvent (ethanol 96%), reaction temperature 60 °C, benzaldehyde/acetophenone: 1.2 molar ratios, reaction time 6 h
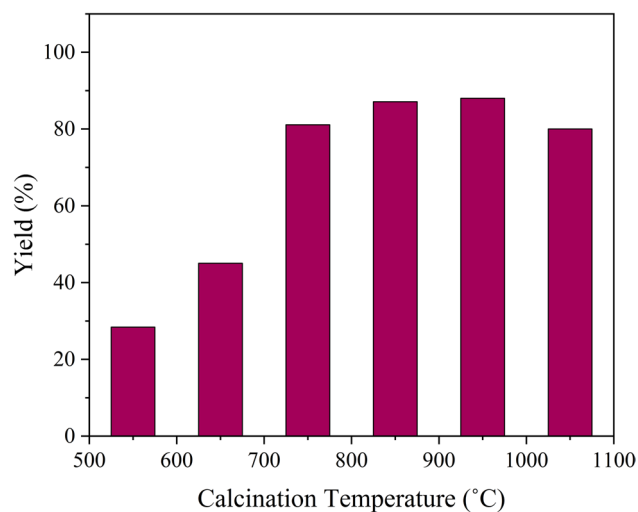
Fig. 8 Effect of calcination temperature. Reaction conditions: 0.04 wt% of $Sr_{0.5}Ca_{2.5}Al$ catalyst, 5 mL solvent (ethanol 96%), reaction time 6 h, benzaldehyde/acetophenone: 1.2, and reaction temperature 60 °C

material toward the catalyst surface decreases, and therefore, the reaction rate is limited by external diffusion. The above results indicated the optimum catalyst amount is around 0.04 wt% (0.09 g).

Effect of molar ratio of raw materials

To evaluate the effect of raw materials' molar ratio on the yield (%) of chalcone, many experiments in the presence of calcined $Sr_{0.5}Ca_{2.5}Al$ catalyst with different molar ratios of benzaldehyde/acetophenone were performed. The reactions were carried out at 60 °C for 6 h using 0.09 g of $Sr_{0.5}Ca_{2.5}Al$ catalyst, 5 mL of solvent (ethanol 96%), and five different molar ratios of benzaldehyde/acetophenone in the range of 0.5–2. According to Fig. 9b, by increasing the molar ratio of benzaldehyde to acetophenone up to 1.2, the yield (%) of chalcone, has also increased. But increasing more than that has not had much effect on the yield percentage. Therefore, 1.2 was chosen as the optimal molar ratio.

Effect of reaction temperature

The reaction was carried out under different temperatures (20–80 °C) in the presence of $Sr_{0.5}Ca_{2.5}Al$ calcined catalyst to check the effect of temperature change on the reaction. The reactions were performed with 0.09 g of catalyst, 1.2 of benzaldehyde/acetophenone molar ratio, 6 h reaction time, and 5 mL of solvent (ethanol 96%). The results in Fig. 10a show that raising the temperature up to 60 °C improved the chalcone yield (%). After this temperature, the yield (%) of chalcone has decreased to a small amount may be due to the
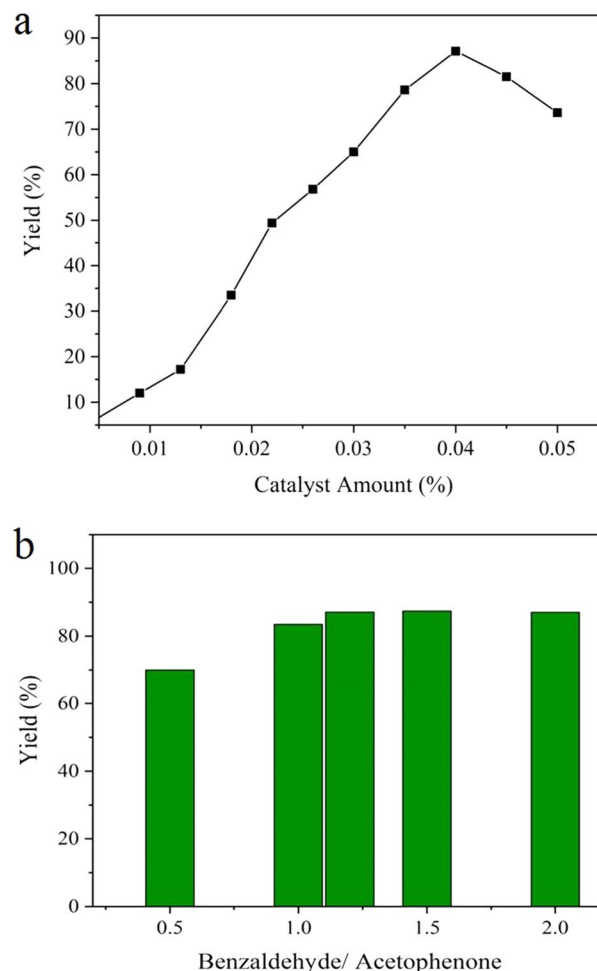
Fig. 9 **a** Effect of the amount of catalyst. [a]Yield of pure isolated chalcone. Reaction conditions: $Sr_{0.5}Ca_{2.5}Al$ calcined at 850 °C as the catalyst, 5 mL solvent (ethanol 96%), reaction time 6 h, benzaldehyde/acetophenone molar ratio: 1.2, and reaction temperature 60 °C. **b** Effect of molar ratio of raw materials. Reaction conditions: 0.04 wt% of Sr0.5Ca2.5Al HT-like calcined at 850 °C as the catalyst, reaction time 6 h, 5 mL solvent (ethanol 96%), and reaction temperature 60 °C

production of side products. Therefore, the proper temperature for this reaction system is around 60 °C.

Effect of reaction time

To determine the minimum time required for the condensation reaction between acetophenone and benzaldehyde to achieve the highest yield (%) of chalcone, the effect of reaction time was, studied. The reactions were carried out in the presence of 0.09 g of $Sr_{0.5}Ca_{2.5}Al$ HT-like calcined at 850 °C as the catalyst, using 5 mL of solvent (ethanol 96%), reaction temperature 60 °C, 1.2 molar ratios of benzaldehyde/acetophenone, and reaction time in the range of 2–24 h. According to Fig. 10b, increasing the reaction time up to 6 h has increased the yield (%) of chalcone to the maximum
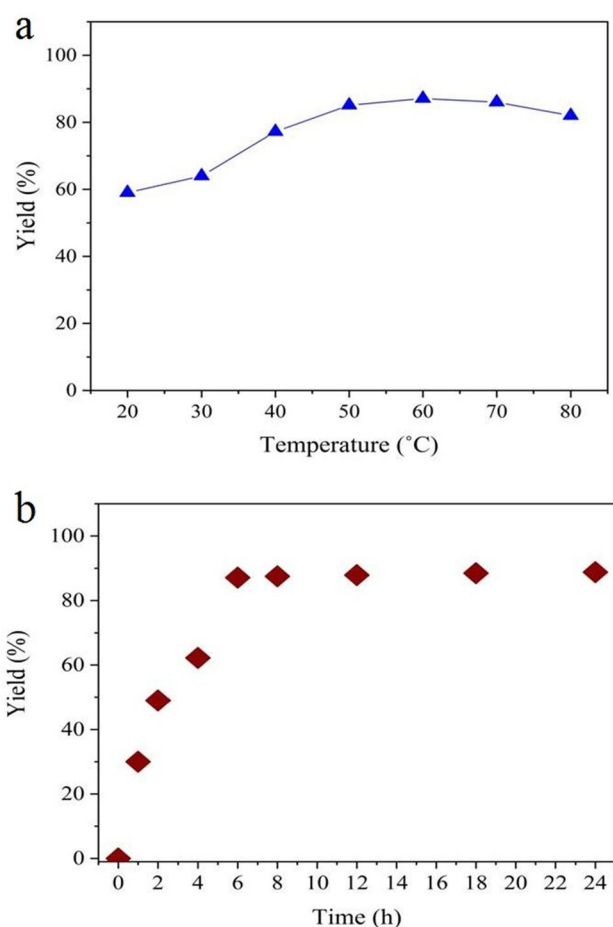
Fig. 10 **a** Effect of reaction temperature. Reaction conditions: 0.09 g of $Sr_{0.5}Ca_{2.5}Al$ HT-like calcined at 850 °C as the catalyst, 5 mL solvent (ethanol 96%), benzaldehyde/acetophenone: 1.2 molar ratios, and reaction time 6 h. **b** Effect of reaction time. Reaction conditions: 0.04 wt% of $Sr_{0.5}Ca_{2.5}Al$ HT-like calcined at 850 °C as the catalyst, 5 mL solvent (ethanol 96%), benzaldehyde/acetophenone: 1.2 molar ratios, and reaction temperature 60 °C

value of 87%, and above this time, the yield (%) of chalcone remained almost constant. Therefore, the equilibrium time of 6 h is suitable for the desired reaction.

Effect of solvents

To evaluate the solvent effect on the yield (%) of chalcone, many experiments were performed with various solvents while the other conditions (0.09 g of the $Sr_{0.5}Ca_{2.5}Al$ catalyst, benzaldehyde/acetophenone: 1.2 molar ratios, reaction temperature 60 °C, reaction time 6 h) have remained the same (see Table 4). Initially, the reaction was performed under solvent-free conditions and did not progress significantly. Also, the reaction did not progress much under a non-polar solvent. Then, polar green solvents of water and ethanol mixture with different (V/V) ratios were used for this reaction. According to Table 4, the reaction in the presence of ethanol had a better efficiency, and ethanol with 96% purity had a better than 99%. It was found that a very small amount of water is useful to advance the reaction. Also, doubling and tripling the amount of solvent does not have a great effect on increasing the yield of chalcone production, so, 5 mL of 96% ethanol is suitable for this reaction.

Catalyst reusability

For reusability study, after the reaction was completed, the $Sr_{0.5}Ca_{2.5}Al$ calcined catalyst was separated from the reaction blend, washed several times with ethanol, and carefully dried in the oven to reuse the catalyst in the reaction and also to study its lifetime and stability. According to Table 5, the $Sr_{0.5}Ca_{2.5}Al$ HT-like catalyst has been used up to four times in the reaction, while about 2% of the yield (%) of chalcone has decreased. The X-ray diffraction profiles and FT-IR analysis were taken from the recycled catalyst after being used up to four times (See Fig. 11). These results show

Table 4 Effect of solvent on the Claisen–Schmidt condensation reaction between acetophenone and benzaldehyde in the presence of $Sr_{0.5}Ca_{2.5}Al$ HT-like catalyst

Solvent	Volume (mL)	H_2O (V/V%)	Relative polarity	Yield[a] (%)
without	0	0	–	6.6
H_2O	5	100	1	12
EtOH(99%): H_2O(1:4)	5	81	0.93	33.8
EtOH(99%): H_2O(2:3)	5	61	0.86	71.1
EtOH(99%):H2O(1:1)	5	51	0.83	75.9
EtOH(99%): H_2O(3:2)	5	41	0.79	79.4
EtOH(99%): H_2O(4:1)	5	21	0.72	83.4
EtOH(99%)	5	1	0.65	80
EtOH(96%)	5	4	0.67	87.1
EtOH(96%)	10	4	0.67	88
EtOH(96%)	15	4	0.67	87.7

[a]Yield of pure isolated Chalcone, Reaction conditions: 0.04 wt % of $Sr_{0.5}Ca_{2.5}Al$ HT-like calcined at 850 °C as the catalyst, reaction time 6 h, benzaldehyde/acetophenone: 1.2 molar ratios, and reaction temperature 60 °C

Table 5 Reused of the recovered catalyst

Number of cycles	Yield[a] (%)
1	87.1
2	86.7
3	86.3
4	85.8
5	85.2

[a]Yield of pure isolated Chalcone, Reaction conditions: 0.04 wt% of $Sr_{0.5}Ca_{2.5}Al$ calcined catalyst at 850 °C, 5 mL solvent (ethanol 96%), reaction time 6 h, benzaldehyde/acetophenone: 1.2 molar ratios, and reaction temperature 60 °C

that the $Sr_{0.5}Ca_{2.5}Al$ HT-like catalyst is completely stable and has preserved its structure.

Claisen–Schmidt condensation reaction on different catalytic systems

Claisen–Schmidt condensation reaction with acetophenone and benzaldehyde on different catalytic systems is given in Table 6. As it can be seen, the $Sr_{0.5}Ca_{2.5}Al$ HT-like catalyst, while being simple and cheap, has high activity in the reaction under mild conditions, and it can be seen that this catalyst has a catalytic activity comparable to other catalytic systems, therefore, this catalytic system is suitable for Claisen–Schmidt condensation. Other catalysts with good activity such as the Cs–pollucite catalyst have been investigated under severe reaction conditions and have a complex synthesis [55].

Effect of substituent on the preparation of chalcones

The effect of using different substituted benzaldehydes and acetophenone in the synthesis of chalcones was studied, the results of which are reported in Table 6. It is well understood that the presence of electron-withdrawing groups (Cl, NO_2) on benzaldehyde and acetophenone (Entry 2, 5) has influenced the formation of enolate form and the yields of resulting chalcones. Also, electron-donating groups (OH, CH_3, OCH_3) have slightly reduced efficiency. Although both electron-donating and electron-withdrawing groups have reacted with appropriate efficiency, the presence of electron-withdrawing groups creates partial positive effects. According to Table 7, excellent yields have been obtained with benzaldehydes that have Cl electron-withdrawing groups (Entry 2), and the lowest efficiency has been obtained with acetophenone which has a methoxy group (Entry 6) (which is a strong resonant electron-donating group).

Suggested mechanism of Claisen–Schmidt condensation reaction

The chalcone synthesis reaction as a green process was carried out at atmospheric pressure and 60 °C, in ethanol (96%) as solvent. At first, acetophenone is treated with the HT-like solid base catalyst that converts it to a more active enolate form. In the next step, it reacts with benzaldehyde to form an intermediate (Scheme 2). In the last step, with a heat of 60 ºC and in the presence of the catalyst, by removing a molecule of water, a conjugated double bond with carbonyl is created and the product becomes thermodynamically more stable [5].
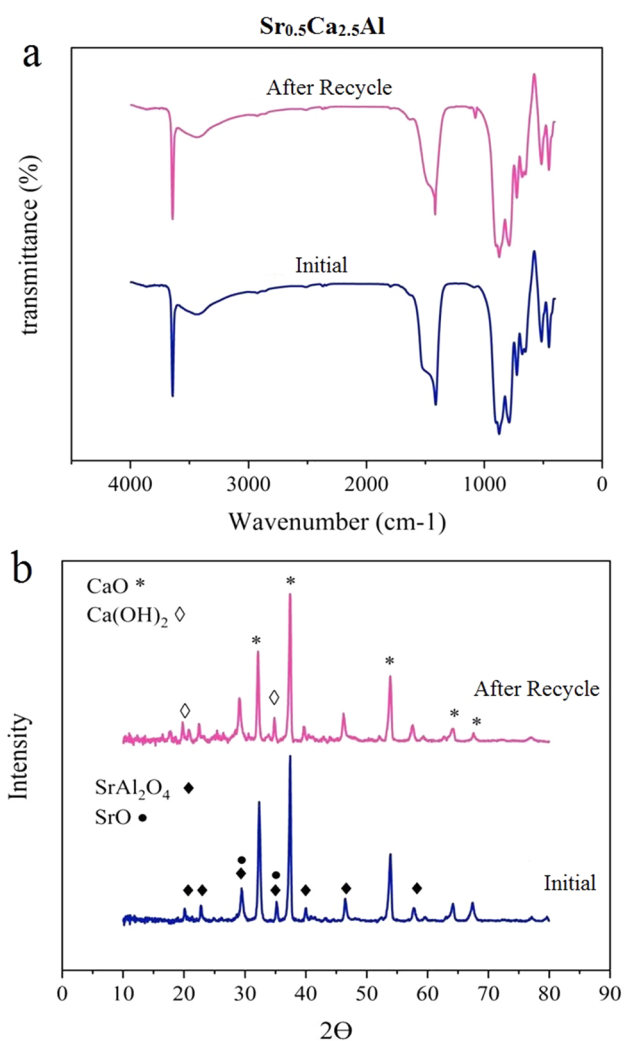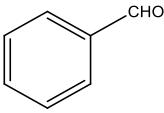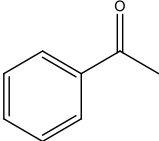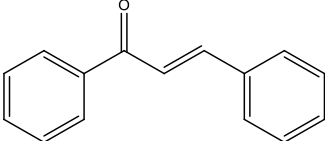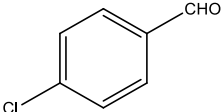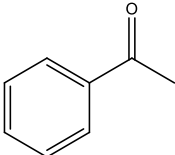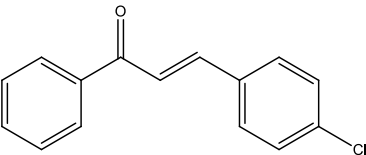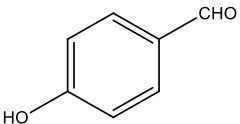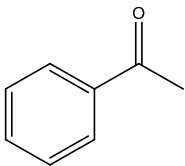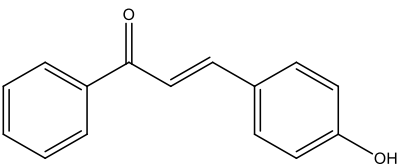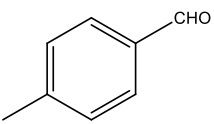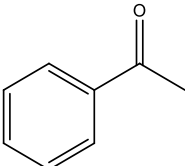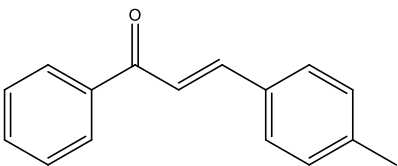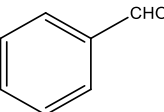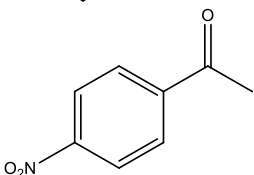

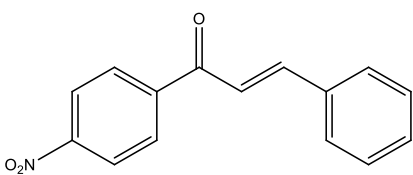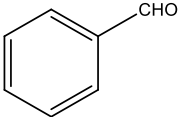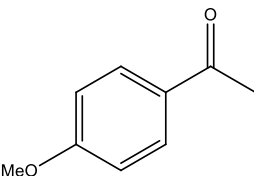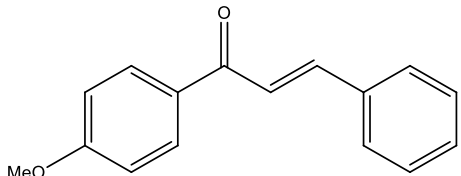**Fig. 11** **a** FT-IR, and **b** XRD pattern of $Sr_{0.5}Ca_{2.5}Al$ HT-like catalyst after calcination, and after recycling
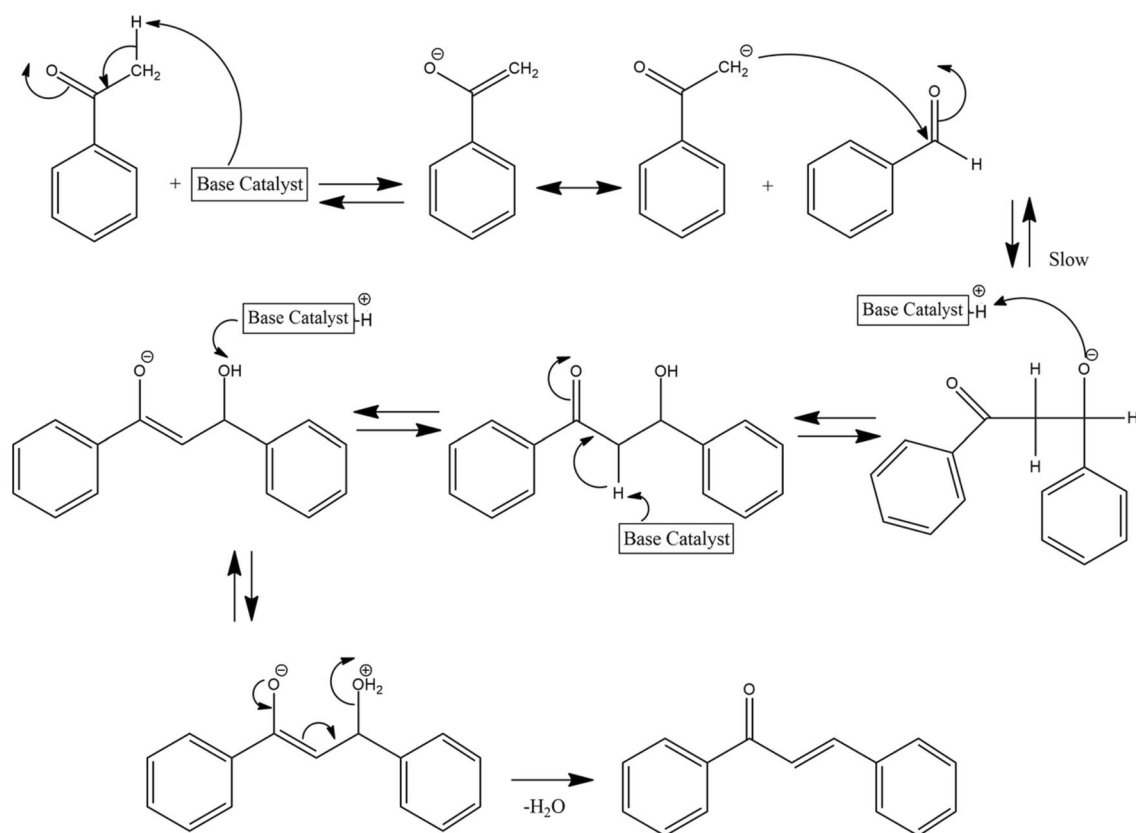
Table 6 Claisen–Schmidt condensation reaction on different catalytic systems

Catalyst	Solvent	Temperature (°C)	Time (h)	Yield (%)	References
$Sr_{0.5}Ca_{2.5}Al$ HT-like	EtOH	60	6	87.1	Our catalyst
Zn-Al HT	–	140	6	41.1	[4]
LDH-rGO	ACN	40	8	75	[18]
CBr_4	EtOH	60	24	77	[10]
IRMOF-3	DMSO	140	24	78	[56]
Cs–pollucitenano zeolite	-	200	1.7	82.2	[55]
Na-ACE (sodium impregnated on activated chicken eggshells)	EtOH	60	1	43	[17]

Table 7 Effect of electron-donating and electron-withdrawing groups substituent on the yield (%) of chalcones

Entry	Aldehyde	Ketone	Product	Yield (%) [a]
1				87.1
2				91.4
3				83
4				88.4
5				87.9
6				76.7

[a]Yield of pure isolated product, Reaction conditions: 0.04 wt% of $Sr_{0.5}Ca_{2.5}Al$ calcined catalyst at 850 °C, 5 mL solvent (ethanol 96%), reaction time 6 h, aldehyde/ketone: 1.2 molar ratios, and reaction temperature 60 °C.

Scheme 2 The suggested mechanism of Claisen–Schmidt condensation reaction by mixed metal oxides base catalyst

Conclusions

In this work, we have developed a simple, clean, and efficient solid base catalytic system for the synthesis of chalcones. In this effective process, a series of Ca_3Al hydrotalcite (HT) samples and $Ca_{2.5}M_{0.5}Al$ (M: Sr, Cd, Ni, and Co) HT-like were successfully synthesized and after calcination, was used as a solid base nanocatalyst in the Claisen–Schmidt reaction. Among the synthesized catalysts, the $Sr_{0.5}Ca_{2.5}Al$ sample had the highest activity. This study showed that the replacing of divalent cations M^{2+} with Ca^{2+} in the Ca_3Al mixed oxides derived from LDH precursors creates three types of medium, strong, and stronger basic sites due to the interaction between M, Ca, and Al oxides and the catalytic activity is dependent on the number of stronger basic sites.

Briefly, this catalytic system is non-toxic, inexpensive, convenient, and reusable. This system was used in mild conditions, with atmospheric pressure and temperature of 60 °C, in a mixture of ethanol and water as a green solvent. The yield (%) of chalcones reached 87% in the presence of 0.04 wt% (0.09 g) of $Sr_{0.5}Ca_{2.5}Al$ catalyst at 60 °C in 6 h.

Author contributions VM helped in supervision, methodology, and conceptualization, ZN is a Ph.D. Student done investigation and writing—original draft preparation. KK contributed to supervision and validation.

Declarations

References

1. P.E. More, B.P. Bandgar, V.T. Kamble, Catal. Commun. **27**, 30–32 (2012). https://doi.org/10.1016/j.catcom.2012.06.012
2. Y. Chinthala, S. Thakur, S. Tirunagari, S. Chinde, A.K. Domatti, N.K. Arigari, K.V. Srinivas, S. Alam, K.K. Jonnala, F. Khan, A. Tiwari, P. Grover, Eur. J. Med. Chem. **93**, 564–573 (2015). https://doi.org/10.1016/j.ejmech.2015.02.027
3. B.E. Aksöz, R. Ertan, Fabad J. Pharm. Sci. **36**, 223–242 (2011)
4. L.B. Kunde, S.M. Gade, V.S. Kalyani, S.P. Gupte, Catal. Commun. **10**, 1881–1888 (2009). https://doi.org/10.1016/j.catcom.2009.06.018

5. M. Álvarez, D. Crivoi, F. Medina, D. Tichit, Chem. Eng. (2019). https://doi.org/10.3390/chemengineering3010029

6. S.L. Gaonkar, U.N. Vignesh, Res. Chem. Intermed. **43**, 6043–6077 (2017). https://doi.org/10.1007/s11164-017-2977-5

7. S. Jain, S. Kumar, B.Y. Lamba, J. Patra, N. Mahindroo, Synth. Commun. **51**, 1–12 (2020). https://doi.org/10.1080/00397911.2020.1817941

8. S. Tripathi, R. Kapoor, L.D.S. Yadav, Adv. Synth. Catal. **360**, 1407–1413 (2018). https://doi.org/10.1002/adsc.201701559

9. D. Kakati, J.C. Sarma, Cent. J. (2011). https://doi.org/10.1186/1752-153X-5-8

10. I. Kazi, S. Guha, G. Sekar, Org. Lett. **19**, 1244–1247 (2017). https://doi.org/10.1021/acs.orglett.7b00348

11. O.A. Shareef, S.A. Said, A.Y. Abdulrazaq, J. Chem. Soc. Pak. **41**, 1046 (2019)

12. R.M. Borade, S.B. Somvanshi, S.B. Kale, R.P. Pawar, K.M. Jadhav, Mater. Res. Express (2020). https://doi.org/10.1088/2053-1591/ab6c9c

13. H. Chaker, G. Ferouani, I. Chikhi, M. Djennas, S. Fourmentin, Coll. Interface Sci. Commun. (2021). https://doi.org/10.1016/j.colcom.2021.100461

14. W. Dan, J. Dai, Eur. J. Med. Chem. (2020). https://doi.org/10.1016/j.ejmech.2019.111980

15. P. Yadav, K. Lal, A. Kumar, S.K. Guru, S. Jaglan, S. Bhushan, Eur. J. Med. Chem. **126**, 944–953 (2017). https://doi.org/10.1016/j.ejmech.2016.11.030

16. A. Hammuda, R. Shalaby, S. Rovida, D.E. Edmondson, C. Binda, A. Khalil, Eur. J. Med. Chem. **114**, 162–169 (2016). https://doi.org/10.1016/j.ejmech.2016.02.038

17. L. Mardiana, B. Ardiansah, R. Bakri, A.H. Cahyana, Y. Anita, N.P. Aziza, Adv. Synth. Catal. **352**, 711–717 (2010). https://doi.org/10.1002/adsc.200900747

18. S. Nasir Abbas Bukhari, M. Jasamai, I. Jantan, W. Ahmad, Mini-Rev. in Org Chem. **10**, 73–83 (2013)

19. A. Dhakshinamoorthy, M. Alvaro, H. Garcia, Adv. Synth. Catal. **352**, 711–717 (2010). https://doi.org/10.1002/adsc.200900747

20. G.D. Yadav, D.P. Wagh, Chem. Sel. **5**, 9059–9085 (2020). https://doi.org/10.1002/slct.202001737

21. U.G.M. Ekanayake, H. Weerathunga, J. Weerasinghe, E.R. Waclawik, Z. Sun, J.M. MacLeod, A.P. O'Mullane, K. Ostrikov, Sustain. Mater. Technol. (2022). https://doi.org/10.1016/j.susmat.2022.e00394

22. A. Navajas, I. Campo, A. Moral, J. Echave, O. Sanz, M. Montes, J.A. Odriozola, G. Arzamendi, L.M. Gandía, Outstanding performance of rehydrated Mg-Al hydrotalcites as heterogeneous methanolysis catalysts for the synthesis of biodiesel. Fuel **211**, 173–181 (2018). https://doi.org/10.1016/j.fuel.2017.09.061

23. T. Jose, J. Ftouni, P.C. Bruijnincx, Catal. Sci. Technol. **11**, 3428–3436 (2021). https://doi.org/10.1039/d1cy00102g

24. C. Sun, F. Qiu, D. Yang, B. Ye, Fuel Process. Technol. **126**, 383–391 (2014). https://doi.org/10.1016/j.fuproc.2014.05.021

25. J. Ashok, Y. Kathiraser, M.L. Ang, S. Kawi, Appl. Catal. B Environ. **172–173**, 116–128 (2015). https://doi.org/10.1016/j.apcatb.2015.02.017

26. Y. Zhang, C. Zhang, S. Xing, J. Solid State Chem. **304**, 122565 (2021). https://doi.org/10.1016/j.jssc.2021.122565

27. K. Kaneda, T. Mizugaki, Green Chem. **21**, 1361–1389 (2019). https://doi.org/10.1039/C8GC03391A

28. A.-E. Stamate, R. Zăvoianu, O.D. Pavel, R. Birjega, A. Matei, M. Dumitru, I. Brezeştean, M. Osiac, I.-C. Marcu, Molecules (2021). https://doi.org/10.3390/molecules26206191

29. W. Bing, H. Wang, L. Zheng, D. Rao, Y. Yang, L. Zheng, B. Wang, Y. Wang, M. Wei, Green Chem. **20**, 3071–3080 (2018). https://doi.org/10.1039/C8GC00851E

30. X. Yu, Int. J. Electrochem. Sci. (2019). https://doi.org/10.20964/2019.01.34

31. R. Karcz, J.E. Olszówka, B.D. Napruszewska, J. Kryściak-Czerwenka, E.M. Serwicka, A. Klimek, K. Bahranowski, Catal. Commun. (2019). https://doi.org/10.1016/j.catcom.2019.105821

32. F.L. Theiss, G.A. Ayoko, R.L. Frost, Appl. Surf. Sci. **383**, 200–213 (2016). https://doi.org/10.1016/j.apsusc.2016.04.150

33. T. Baskaran, J. Christopher, A. Sakthivel, Rsc Adv. **5**, 98853–98875 (2015). https://doi.org/10.1039/C5RA19909C

34. A.R. Sangtam, P. Saikia, R.L. Goswamee, U.B. Sinha, Today Chem. **29**, 101426 (2023). https://doi.org/10.1016/j.mtchem.2023.101426

35. D.K. Yadav, S. Uma, R. Nagarajan, Appl. Clay Sci. (2022). https://doi.org/10.1016/j.clay.2022.106655

36. A.-E. Stamate, O.D. Pavel, R. Zăvoianu, R. Bîrjega, K. Neubauer, A. Koeckritz, I.-C. Marcu, Mol. Catal. **537**, 112968 (2023). https://doi.org/10.1016/j.mcat.2023.112968

37. E.M. Fuentes, J.I. Ruiz, M.D. Santos, Dyna **86**, 58–65 (2019). https://doi.org/10.15446/dyna.v86n210.78559

38. W. Bing, L. Zheng, S. He, D. Rao, M. Xu, L. Zheng, B. Wang, Y. Wang, M. Wei, ACS ACS Catal. **8**, 656–664 (2017). https://doi.org/10.1021/acscatal.7b03022

39. P. Salinas Hernández, F. Morales Anzures, R. Pérez Hernández, F. Tzompzntzi Morales, M.A. Romero Romo, Catal. Today **34**, 948–956 (2020). https://doi.org/10.1016/j.cattod.2018.06.034

40. M. Rosset, L.A. Féris, O.W. Perez-Lopez, Catal. Today **381**, 96–107 (2021). https://doi.org/10.1016/j.cattod.2020.08.018

41. L. Valeikiene, M. Roshchina, I. Grigoraviciute-Puroniene, V. Prozorovich, A. Zarkov, A. Ivanets, A. Kareiva, Crystals (2020). https://doi.org/10.3390/cryst10060470

42. X. Zhou, C. Zhang, ACS Omega **6**, 5056–5060 (2021). https://doi.org/10.1021/acsomega.0c06269

43. F. Janani, H. Khiar, N. Taoufik, A. Elhalil, M. Sadiq, A. Puga, S. Mansouri, N. Barka, Mater. Today Chem. **21**, 100495 (2021). https://doi.org/10.1016/j.mtchem.2021.100495

44. I.Z. Awan, G. Beltrami, D. Bonincontro, O. Gimello, T. Cacciaguerra, N. Tanchoux, A. Martucci, S. Albonetti, F. Cavani, F. Di Renzo, Appl. Catal. A Gen. (2021). https://doi.org/10.1016/j.apcata.2020.117929

45. F. Shahbazi, V. Mahdavi, J. Zolgharnein, J. Iran. Chem. Soc. **17**, 333–349 (2019). https://doi.org/10.1007/s13738-019-01772-6

46. P. Kulkarni, Curr. Microw. Chem. **2**, 144–149 (2015)

47. P.-H. Chang, Y.-P. Chang, S.-Y. Chen, C.-T. Yu, Y.-P. Chyou, Chem. Sus. Chem. **4**, 1844–1851 (2011). https://doi.org/10.1002/cssc.201100357

48. J. Granados-Reyes, P. Salagre, Y. Cesteros, Appl. Catal. A: Gen. **536**, 9–17 (2017). https://doi.org/10.1016/j.apcata.2017.02.013

49. R. Ramos, A.F. Peixoto, B.I. Arias-Serrano, O.S.G.P. Soares, M.F.R. Pereira, D. Kubička, C. Freire, Chem. Cat. Chem. **12**, 1467–1475 (2020). https://doi.org/10.1002/cctc.201902033

50. K. Mehta, M.K. Jha, N. Divya, Res. Chem. Intermed. **44**, 7691–7709 (2018). https://doi.org/10.1007/s11164-018-3581-z

51. F. Teodorescu, A. Slabu, O. Pavel, R. Zăvoianu, Catal. Commun. **133**, 105829 (2020). https://doi.org/10.1016/j.catcom.2019.105829

52. F. Farzaneh, M. Kashani Maleki, E. Rashtizadeh, J. Clust. Sci. **28**, 3253–3263 (2017). https://doi.org/10.1007/s10876-017-1288-8

53. M.P. Bernardo, F.K.V. Moreira, C. Ribeiro, Appl. Clay Sci. **137**, 143–150 (2017). https://doi.org/10.1016/j.clay.2016.12.022

54. W. Chen, Z. Huang, Y. Liu, Q. He, Catal. Commun. **9**, 516–521 (2008). https://doi.org/10.1016/j.catcom.2007.02.011

55. S.A.G. Mohammad, F. Khoerunnisa, S. Rigolet, T.J. Daou, T.C. Ling, E.P. Ng, Processes (2020). https://doi.org/10.3390/pr8010096

56. S. Wu, X. Ma, J. Ran, Y. Zhang, F. Qin, Y. Liu, RSC Adv. **5**, 14221–14227 (2015). https://doi.org/10.1039/C4RA16180G